Developmental Corneal Innervation: Interactions between Nerves and Specialized Apical Corneal Epithelial Cells

James K. Kubilus and Thomas F. Linsenmayer

Purpose. The corneal epithelium is one of the most highly innervated structures in the body, and proper innervation is necessary for corneal maintenance and sensation. However, little is known about how these nerves function and how innervation occurs developmentally. The authors have examined certain aspects of corneal innervation in the developing chicken embryo.

Methods. DiI was used to determine the source of the neurons responsible for innervating the cornea. Immunohistochemistry, electron microscopy, and immunoelectron microscopy were used to examine corneal innervation and the relationships that develop between nerves and corneal epithelial cells.

Results. Corneal nerves in the embryonic chicken originate entirely from the ophthalmic lobe of the trigeminal ganglion. Within the cornea the nerves interact with apical corneal epithelial (ACE) cells to form specialized structures that are synapse-like because they contain accumulations of vesicles and have the SV2 synaptic vesicle protein. These ACE cells themselves have unique characteristics, including transient expression of the neuronal isoform of class III β-tubulin and formation of extensive intercellular channels and clefts that contain these specialized synapse-like structures and nerves; in addition, they are mitotically active. Given that these ACE cells react with a monoclonal antibody against this neuronal isoform of β-tubulin (the TuJ-1 antibody), we have termed them TuJ-1^{+}ACE cells.

Conclusions. During avian corneal development the nerves make close associations with a specialized type of ACE cell. There they form synapse-like structures, suggesting that not all nerves within the CE terminate as free nerve endings. (*Invest Ophthalmol Vis Sci.* 2010;51:782–789) DOI:10.1167/iovs.09-3942

The cornea has several functions. It protects the underlying ocular tissues of the eye, and it focuses light on the retina. Because damage to the cornea or changes in its shape, thickness, or transparency can impair the passage of light, maintaining a healthy cornea is vital for normal vision. One factor involved in this maintenance is innervation. It is known that the cornea is one of the most densely innervated tissues in the body.[1] It is also known that these nerves originate predominantly from the ophthalmic lobe of the trigeminal ganglion (OTG) and that they are predominately afferent sensory nociceptors (i.e., they transduce mechanical, thermal, and chemical stimuli as sensations of pain). They also are involved in protecting the cornea from damage by modulating the blink response and increasing the production of tears and in maintaining the cornea in a healthy state through the production of trophic factors. Thus, any disruption of these nerves (e.g., by viral infection or through trauma or surgical procedures) can have deleterious effects on the integrity and transparency of the cornea.[2,3]

Despite the importance of corneal nerves, surprisingly little is known concerning the mechanisms involved in corneal innervation, either during normal development or after injury/laser refractive surgery, and even less is known concerning the subsequent interaction(s) between corneal nerves and corneal epithelial (CE) cells.

For developmental studies of corneal innervation, the chicken embryo provides an advantageous model. As described originally by Bee et al.,[4,5] in this species innervation occurs as a series of discrete stages temporally and spatially separate from one another. These stages involve the growth and attraction of nerves from the OTG to the cornea, the formation of a ring of nerves (the pericorneal ring) surrounding the cornea but not entering it, the subsequent centripetal invasion of nerves from this ring into the corneal stroma, and the turning of nerves toward the corneal surface and their penetration through Bowman's layer into the corneal epithelium. Concerning the mechanisms involved in regulating these stages, again, little is known. However, recent work[6] (JKK and TFL, unpublished observations, 2007) has strongly suggested an involvement of the axon guidance cue Semaphorin3A on the initial stages of corneal innervation, particularly during formation of the pericorneal ring and the subsequent invasion of nerves into the stroma.

Another unknown is whether nerves and CE cells interact directly with one another (e.g., in transducing noxious stimuli to sensations of pain and in providing trophic support to the corneal epithelium). However, some evidence for such interactions exists. In vitro studies making use of cocultures of trigeminal neurons and CE cells suggest that these two cell types do support one another through the secretion of trophic factors.[7–10] In addition, studies of corneas after photorefractive keratectomy or LASIK have suggested a decrease in innervation of the corneal epithelium that correlates with postsurgical complications such as corneal opacification[11] and LASIK-induced neurotrophic epitheliopathy.[12]

It is generally thought that afferent nociceptive nerves, such as those that innervate the corneal epithelium, terminate as simple free nerve endings; however, some ultrastructural observations in rabbits and humans have shown a close relation-

From the Program in Cell, Molecular and Developmental Biology, Sackler School of Graduate Biomedical Sciences, Department of Anatomy and Cellular Biology, Tufts University School of Medicine, Boston, Massachusetts.

Supported by National Institutes of Health Grant 1R01EY018889–01A1 and Training Grant 5T32-HD007403–14 (JKK).

Submitted for publication May 1, 2009; revised June 24, 2009; accepted October 26, 2009.

Disclosure: **J.K. Kubilus**, None; **T.F. Linsenmayer**, None

Corresponding author: Thomas F. Linsenmayer, 750 Washington Street, Box SCH, Boston, MA 02111; thomas.linsenmayer@tufts.edu.

ship between nerves and CE cells, as might be expected for a more complex type of nerve cell interaction.[13,14]

In the present study, using the embryonic chicken cornea as a model, we examined corneal nerves and CE cells after all the stages of innervation were completed. Through a combination of electron and confocal microscopy, we observed that the corneal nerves formed complex structures with ACE cells. Furthermore, these structures, by immunohistochemistry using confocal immunofluorescence and immunoelectron microscopy, contain the neuronal marker protein class IIIβ-tubulin (as determined using the TuJ-1 antibody) and the synaptic vesicle component SV2 (as determined using the SV2 antibody). In addition, only ACE cells involved in the formation of these complex structures, but no other CE cell type, reacted with the TuJ-1 antibody, suggesting that they represent a unique type of CE cell involved in innervation that we have termed the TuJ-1$^+$ ACE cell.

Methods

Animals

Chicken eggs (White Leghorn) were obtained from Hyline (Elizabethtown, PA) and incubated at 38°C. Embryos were removed, rinsed in Hank's balanced saline solution (Invitrogen, Carlsbad, CA), and staged both by chronological time of incubation and by the criteria of Hamburger and Hamilton.[15]

Retrograde DiI Labeling of Corneal Nerves

Retrograde labeling of the cell bodies of nerves that innervate the cornea was performed according to Fujimori.[16] Briefly, embryonic day (E14 chicken embryos were removed from eggs and decapitated. The heads were placed in Hank's balanced saline solution (Invitrogen), the eyelids were surgically removed with iridectomy scissors, and a small crystal of DiI (1,1′-dioctadecyl-3,3,3′,3′-tetramethylindocarbocyanine perchlorate; Molecular Probes, Eugene, OR) was placed on the center of the corneal surface of the left eye using a fine tungsten needle. The right eye served as an unlabeled control. The head was then gently placed in freshly made paraformaldehyde (4% in 0.1 M PBS, pH 7.4) and kept at 37°C in the dark for 2 months. After this the head was transferred to 0.1 M PBS, and both the left and right trigeminal ganglia, the superior cervical ganglia, and the ciliary ganglia were removed and photographed under a fluorescent dissecting stereomicroscope (SMZ 1500; Nikon Instruments, Melville, NY) equipped with a real-time charge-coupled device (CCD) camera (SPOT Flex; Diagnostic Instruments, Inc., Sterling Heights, MI).

Immunohistochemistry

For IHC of tissue sections, tissues were fixed (4% paraformaldehyde [PFA] in 0.1 M PBS, pH 7.4) for 1 hour to overnight, depending on tissue thickness, and then were processed for either frozen or paraffin sectioning.

For frozen sectioning, after PFA fixation the tissues were cryoprotected (20% sucrose overnight at 4°C) and then embedded in OCT compound (TissueTek; Sakura Finetek USA., Inc., Torrance, CA). Ten-micrometer serial sections were cut using a cryostat. Sections were mounted on poly-L-lysine–coated slides and were then air dried (2 hours at room temperature) and stored (at −20°C). For fluorescence IHC, the sections were rinsed (three times in PBS) and then incubated in blocking solution (10% heat-inactivated sheep serum in PBS with 0.1% Triton X-100) for 1 hour at room temperature. For labeling, the SV2 antibody monoclonal antibody (developed by Kathleen M. Buckley and obtained from the Developmental Studies Hybridoma Bank under the auspices of the National Institute of Child Health and Human Development and maintained by the Department of Biology, University of Iowa, Iowa City, IA) was used undiluted. Antibody (TuJ-1; R&D Systems, Minneapolis, MN) was diluted to 5 μg/mL (in 1% blocking solution). Control corneas were incubated either in blocking solution without primary antibody or in the AC-9 antibody to type X collagen.[17] After incubation in primary antibody (overnight at 4°C), slides were washed (three times for 5 minutes each in PBS) and then incubated (for 1 hour at room temperature in the dark) in anti-mouse red secondary antibody (NorthernLights; R&D Systems; diluted 1:200 in PBS). Nuclei were stained with Hoechst and then were washed (three times in PBS). Slides were then mounted in 95% glycerol in PBS.

For paraffin sections, the PFA-fixed tissues were dehydrated through a graded series of ethanol and then were cleared in xylene (two times for 15 minutes each) and transferred to paraffin (58°C overnight). Tissues were transferred to fresh paraffin (1 hour at 58°C) and were mounted as blocks and cooled and stored at room temperature until sectioned (10 μm). The sections were mounted on poly-L-lysine–coated slides that were then dried on a slide warmer (at 38°C) and stored at 4°C. IHC was performed similar to that for frozen sections, except that before labeling with the antibody (TuJ-1; R&D Systems) an antigen retrieval step was performed. For this the slides were deparaffinized in xylene, rehydrated through a graded series of ethanol to PBS, transferred to sodium citrate buffer (0.1 M, pH 6.5), and boiled in a microwave oven (two times for 5 minutes each at 50% power). Slides were allowed to cool for 20 minutes and then were rinsed twice in H_2O and three times in PBS. Antibody labeling was performed as described for the frozen sections.

The sections were visualized by conventional immunofluorescence microscopy (Fluophot; Nikon Instruments), equipped with a real-time CCD camera (SPOT RT; Diagnostic Instruments, Inc.) and by confocal microscopy using a laser scanning microscope and detector (Zeiss LSM510; Carl Zeiss MicroImaging, Inc., Thornwood, NY).

Whole Mount Immunohistochemistry

For whole mount IHC, the methods of Sillitoe and Hawkes[18] were adapted. Briefly, corneas were fixed for 1 hour in 4% PFA in 0.1 M PBS, followed by overnight fixation in Dent's fixative (4:1 methanol/dimethyl sulfoxide). Corneas were subjected to freeze-thaw (four times in 100% methanol), washed three times in PBS, and transferred to blocking solution (10% heat-inactivated sheep serum in PBS with 0.1% triton X-100) for 24 to 48 hours at 4°C. After blocking, the corneas were incubated in antibody (TuJ-1 [R&D Systems] diluted to 0.5 μg/mL in 10% blocking solution) for 72 hours at 4°C. Control corneas were incubated either in the blocking solution without primary antibody or in the AC-9 antibody to type X collagen.[17] After washing (four changes of PBS over 24 hours at 4°C), the corneas were incubated in secondary antibody (donkey anti-mouse Northern Lights red [R&D Systems] diluted 1:200 in PBS at 4°C for 48 hours.). The corneas were washed again (in four changes of PBS over 24 hours) and then incubated in Hoechst (for 24 hours at 4°C) to stain nuclei. After washing (two times in PBS over 24 hours at 4°C), the corneas were mounted on poly-L-lysine–coated slides (Fisher Scientific, Pittsburgh, PA) in 95% glycerol and stored at 4°C. The samples were visualized by conventional immunofluorescence microscopy (Fluophot; Nikon Instruments, equipped with a real-time CCD camera (SPOT RT; Diagnostic Instruments, Inc.) and by confocal microscopy using a laser scanning microscope and detector (Zeiss LSM510; Carl Zeiss MicroImaging, Inc.).

RT-PCR

For RT-PCR analyses of class III β-tubulin, mRNA was isolated from OTG and from CE tissue (removed from corneas by incubation in Dispase[19]), using an mRNA isolation kit (Microfast-track; Invitrogen). cDNA was reverse transcribed with reverse transcriptase (SuperScript; Invitrogen). Forward (5′-AAC AAT GTC AAG GTG TGC-3′) and reverse (5′-ACT GCT CTG AGA TGC GCT TGA AGA-3′) primers were used to amplify a 163-bp product by PCR, followed by electrophoresis on an ethidium bromide agarose gel and visualization by ultraviolet light illumination.

Electron Microscopy

Corneas were harvested from embryos (E12-E17), fixed in 2% PFA, 2.5% glutaraldehyde in pH 7.3 cacodylate buffer, and postfixed in 1% buffered osmium tetroxide. After dehydration with ethanol and propylene oxide, the tissues were embedded in resin (Epon 812; Shell Chemical, Deer Park, TX). Sections were cut at 70 to 90 nm and were stained with 2% uranyl acetate and Sato's lead stain. Sections were viewed, and the images were captured on an electron microscope (CM-10; Philips, Eindhoven, The Netherlands) run at 80 kV.

Immunoelectron Microscopy

Frozen sections on slides were processed for immunofluorescence through the primary antibody incubation step, as described. They were then incubated in 10 nm gold-conjugated mouse IgG secondary antibody (Sigma-Aldrich, St. Louis, MO; diluted 1:20) for 1.5 hours at room temperature in the dark. Sections were rinsed in 0.1 M sodium cacodylate buffer and fixed overnight in 2.5% glutaraldehyde (at 4°C), and, after another rinse in buffer, they were postfixed in 1% osmium tetroxide in 0.1 M cacodylate buffer (for 1 hour), dehydrated in ethanol, and embedded in resin (Epon-Araldite; Shell Chemical). Sections were then cut, stained with 2% uranyl acetate, and imaged (as described).

Results

DiI Retrograde Labeling

The sensory fibers that innervate the cornea originate chiefly from the OTG. However, in some species (e.g., cats and rabbits), a portion of the corneal nerves reportedly originate from the superior cervical ganglion (SCG).[20] Given that the present studies on corneal innervation were performed using the chicken embryo and that the ganglionic origins of the nerves in this species have not been reported previously, we first determined whether, in this species, all the corneal nerves originate from the OTG or whether these also originate from multiple ganglia.

To determine this we performed retrograde transport using DiI, a lipophilic fluorescent tracer that can be used to establish the origin(s) of the nerves that innervate a target tissue.[16] DiI exhibits weak fluorescence in an aqueous environment; however, when it is incorporated into a lipid membrane, it becomes highly fluorescent and photostable. Once incorporated, the DiI diffuses laterally throughout the cell membrane; diffusion across membranes is thought to occur only if the membranes are continuous and fused or if adjacent cells have specialized structures in which their membranes are in close apposition, such as at tight junctions.[21]

The diffusion of DiI occurs even in paraformaldehyde-fixed tissues, so fixed tissue was used in the present study. For these analyses, a crystal of DiI was placed on the surface of the central cornea of E14 embryos (Fig. 1A, arrow), a developmental stage that occurs several days after nerves reach the ACE cells. Then, we examined whether DiI applied to the corneal surface in such a manner would enter the nerve fibers and undergo retrograde diffusion to the cell bodies within the ganglia and, if so, whether all the labeled neuronal cell bodies would be in the OTG.

Empirically, labeling of the ganglionic nerve cell bodies required extended incubation of the tissues (2 months in 4% paraformaldehyde at 37°C). By this time, whole mount preparations, even as viewed by bright-field (no-fluorescence) microscopy, showed that the dye had spread from the central crystal outward to the periphery of the cornea. Fluorescence microscopy of such whole mounts confirmed the labeling of the cornea (Fig. 1B) and showed labeled nerves exiting the cornea into the sclera (demarcated by the arrows in Fig. 1B and in the enlargement shown in Fig. 1B, inset b″). However, no other structure in the anterior eye was labeled. Sectioned eyes (Fig. 1B, inset b′) showed that within the cornea, the dye was distributed throughout the corneal epithelium but was not in the corneal stroma, scleral epithelium, or stroma.

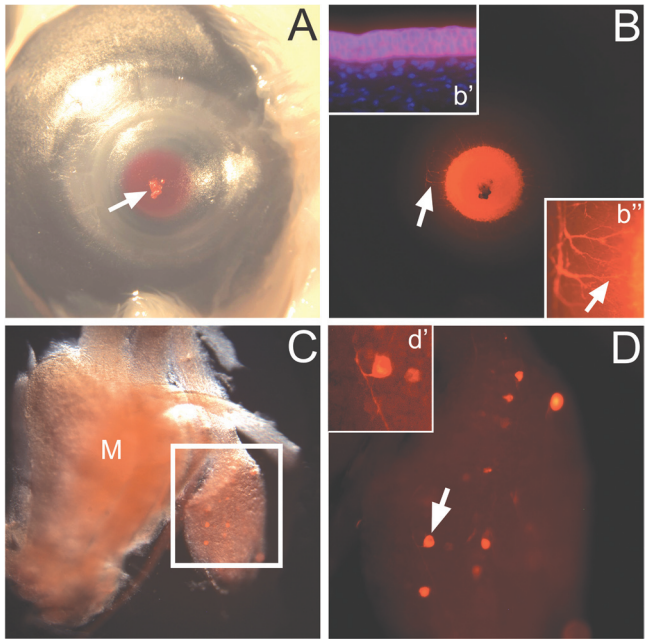

Figure 1. (**A**) Bright-field image of E14 eye with a crystal of DiI (*arrow*) placed in the central cornea. (**B**) Fluorescent image of (**A**) showing DiI diffusing through cornea and into nerves (*arrow*), with higher magnification of nerves (**b″**). (**b′**) Frozen section of DiI-labeled cornea. DiI (*red*) diffused throughout corneal epithelium. (**C**) Bright-field image of TG overlaid with fluorescent image. *Box*: labeled DiI neurons in the OTG but not in mandibular-maxillary lobe (M). (**D**) High-power view of OTG from (**C**) shows DiI-labeled pseudounipolar (**d′**) neurons localized in different regions of the ganglion.

The retrograde DiI labeling of the neuronal cell bodies within the cranial ganglia was then examined. Fluorescently labeled cell bodies were observed only in the OTG. This can be seen in Figure 1C, which is a fluorescent image of an entire trigeminal ganglion overlain with a bright-field image of the same ganglion. Within the trigeminal ganglion, all the DiI-labeled cell bodies are located within the ophthalmic lobe (demarcated with a box), with none detected in the mandibular/maxillary lobe (M). Figure 1D is a enlargement of the fluorescent image of the box in Figure 1C, showing the characteristic pseudounipolar cell bodies indicative of peripheral sensory nociceptive neurons (demarcated by the arrow, and further enlarged in Fig. 1D, inset d′). No DiI labeling was observed in any of the other cranial ganglia examined, including the SCG, or the ciliary, pterygopalatine, submandibular, or otic ganglia.

These results show, in the chicken embryo, that DiI placed on the surface of the corneal epithelium will enter the corneal nerves (see also Discussion) and that the corneal nerves originate solely from the OTG.

TuJ-1$^+$ Apical Corneal Epithelial Cell

For developmental studies of the stages of corneal innervation (Kubilus and Linsenmayer, manuscript in preparation), we adapted a whole mount immunohistochemical procedure[18] making use of a monoclonal antibody specific for the C terminus of class III β-tubulin (the TuJ-1 antibody[22]). Because class

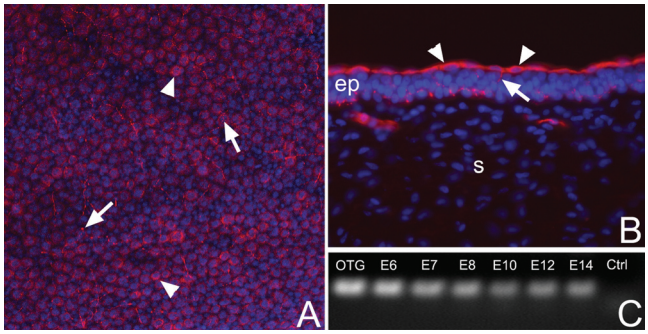

FIGURE 2. (**A**) One-micrometer-thick confocal optical section of corneal surface of whole mount fluorescent TuJ-1 (*red*)-immunolabeled E14 cornea imaged en face with ACE cells (*arrowheads*) and punctate nerve structures (*arrows*). (**B**) Frozen TuJ-1-labeled (*red*) sections with labeled ACE cells (*arrowheads*) and nerves (*arrow*; Hoechst-stained nuclei, *blue*). (**C**) RT-PCR for class III β-tubulin mRNA in corneal epithelium: *Lane 1*, E6 OTG; *lane 2*, E6 corneal epithelium; *lane 3*, E7 corneal epithelium; *lane 4*, E8 corneal epithelium; *lane 5*, E10 corneal epithelium; *lane 6*, E12 corneal epithelium; *lane 7*, E14 corneal epithelium; *lane 8*, no template control. Bands migrate at 163 bp.

III β-tubulin is considered to be nerve-specific, this antibody has been used extensively as a neuronal marker.[23,24]

In analyzing whole mount preparations of embryonic corneas labeled with the TuJ-1 antibody (viewed en face by confocal microscopy; Fig. 2A), we unexpectedly observed that this antibody, in addition to labeling nerves (arrows), also labeled cells within the corneal epithelium (arrowheads). The TuJ-1 labeled cells seemed to be in the ACE cell layer, a location that was confirmed using sectioned corneas from embryonic stages E6 to E16. Figure 2B shows a section of E14 cornea labeled with the TuJ-1 antibody (red) and with the nuclei stained with Hoechst dye (blue). In this section, it is clear that the ACE cells are the only cells labeled by the antibody (arrowheads); thus, we have termed these the TuJ-1$^+$ ACE cells. The other TuJ-1 labeling in this section is in the nerves in the epithelium (ep) and stroma (s). In the epithelium, some of the nerves appear to terminate in punctate structures at the base of the TuJ-1$^+$ ACE cells (arrow), suggesting the possibility of an interaction between the nerves and these cells. No fluorescence was observed in control whole corneas or sections incubated either without primary antibody or with an antibody against type-X collagen (not shown).

Although the β-tubulin family of proteins is highly conserved, both among family members and across species, it is unlikely that the TuJ-1 labeling in the TuJ-1$^+$ ACE cells resulted from cross-reactivity with another β-tubulin rather than the class III neuronal type. First, the β-tubulins do have differences in their amino acid sequences, specifically in their C-terminal region, where the TuJ-1 epitope is located.[22,25] In addition, we have observed by RT-PCR that mRNA for class III β-tubulin is expressed by CE tissue over the developmental period examined (E6-E14; Fig. 2C). Of importance to these analyses, we have observed that during corneal development, TuJ-1 labeling of the TuJ-1$^+$ ACE cells appears at E6, 4 days before nerves enter the corneal epithelium (at E10) (JKK and TFL, unpublished observations). This provides a window during which CE tissue can be analyzed in the absence of nerves, thus eliminating any potential neuronal involvement in the analyses. For these analyses, we used primers designed to be specific for the C-terminal sequence of class III β-tubulin (see Materials and Methods, Sullivan et al.,[25] and Hasegawa et al.[26]). As a positive control and for each age (E6-E14) of corneal epithelium tested, the same stage OTG was run, because the DiI labeling results show that the cell bodies of all the corneal nerves reside there. With cDNA from all ages of corneal epithelium examined, including the critical time period when nerves are absent (E6-E8), and with cDNA from the corresponding OTG (only one of which is shown, Fig. 2C), a PCR product of the appropriate size (163 bp) was observed.

Nerve-TuJ-1$^+$ ACE Cell Interactions

As described, in TuJ-1-labeled whole mount preparations and in sectioned corneas, when nerves have reached the TuJ-1$^+$ ACE cells, there appears to be a close association between the nerves and the basal regions of these cells, which includes the formation of TuJ-1-labeled punctate structures. Corneal nerves are generally thought to terminate as free nerve endings,[13,14] but this is a nebulous term, and a definitive characterization of what constitutes a free nerve ending is lacking (reviewed by Kruger et al.[27]). However, in the nerves of the developing chicken cornea, the presence of these punctate structures suggested a more complex nerve ending. Therefore, we examined this further, initially by confocal microscopy and subsequently by electron and immunoelectron microscopy.

For confocal microscopy, whole corneas were labeled with the TuJ-1 antibody, and nuclei were stained with Hoechst. The corneas were then imaged en face as a Z-series of 1-μm optical sections, starting at the apical-most surface of the corneal epithelium and progressing downward. Figure 3 shows four images from the Z-stack of an E12 cornea, generated over a thickness of 28 μm that spanned the entire corneal epithelium; the arrows in Figures 3A to 3C designate the corresponding region in each image. Figure 3A shows TuJ-1$^+$ ACE cells, many of which have associated fine nerves with punctate structures (e.g., the cell demarcated by the arrow). Because this optical section is 1 μm thick and the thickness of the squamous TuJ-1$^+$ ACE cells themselves is only approximately 1 to 2 μm, this result demonstrates a close association between these cells and the nerves. A corresponding image (Fig. 3B) taken slightly deeper (3 μm) in the corneal epithelium confirms that the punctate structures are located near the base of the TuJ-1$^+$ ACE

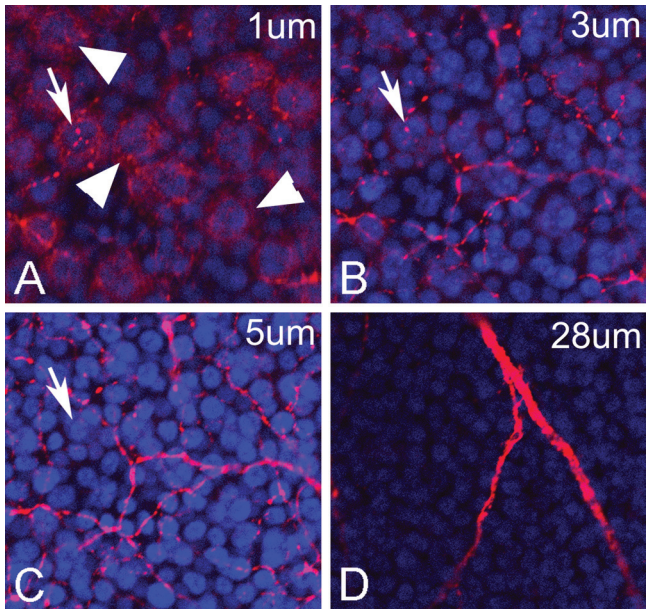

FIGURE 3. (**A**) Confocal optical section of TuJ-1 (*red*)-labeled whole E12 cornea imaged en face at 1 μm shows ACE cells (*arrowheads*), punctate nerve structures (*arrow*), and nuclei (*blue*). (**B**) Optical section at 3 μm with labeled punctate structures (*arrow*). (**C**) Loss of punctate structure at a depth of 5 μm (*arrow*). (**D**) At 28-μm thickened nerve fibers in deeper levels of the cornea.

because at this level, much of the cytoplasmic labeling of the cells is lost, but the labeling of many of the punctate structure remains (e.g., at the arrow).

Optical sections taken progressively more deeply in the corneal epithelium (5 μm, Figs. 3C [28 μm], D) show a complete loss of the TuJ-1 labeling of the cells and a great decrease, or complete loss, of the labeled punctate structures. For the nerves themselves, this progression involves a decrease in number and an increase in diameter.

Immunohistochemistry with the SV2 (Synaptic Vesicle 2) Antibody

That the terminal branches of the nerves in the corneal epithelium have these punctate structures suggests that if the nerves terminate as free nerve endings they are highly specialized ones. Alternatively, these punctate structures may represent specialized nerve endings such as the synapse-like structures described in other organs, which function as specialized transducers of sensation[28] (see Discussion).

If these punctate structures are synapse-like, they should have synaptic components and structures such as vesicles. To examine this possibility, we performed immunohistochemistry using a monoclonal antibody (SV2) directed against the synaptic vesicle 2 protein, both for immunofluorescence (described here) and immunoelectron microscopy (described later). The SV2 protein is a transmembrane glycoprotein that is a conserved component of synaptic vesicles in all vertebrate species examined. The SV2 antibody[29] recognizes both isoforms of this protein[30] and has been widely used as a marker for different types of synaptic vesicles.[31] It also reacts with vesicles undergoing transport through nerves.

Figure 4 shows a fluorescence micrograph of a section from an E16 cornea reacted with the SV2 antibody. At the basal surface of the ACE are labeled, punctate structures (arrow) that have the same distribution and appearance as the punctate structures that label with the TuJ-1 antibody. Most SV2 labeling is aggregated within the large punctate structures at the base of the ACE cells, suggesting that the vesicles accumulate there. However, the antibody labels portions of the nerves themselves, both the thick bundles adjacent to Bowman's layer and the thinner branches coursing toward the apical surface, which is indicative of vesicles undergoing transport. Again, no fluorescence was observed in control sections (not shown).

Ultrastructure of the ACE Cells and Their Relationship with the Synapse-like Structures

To elucidate further the characteristics of the ACE cells and the putative synapse-like structures, and their possible relationships to one another, we used electron and immunoelectron

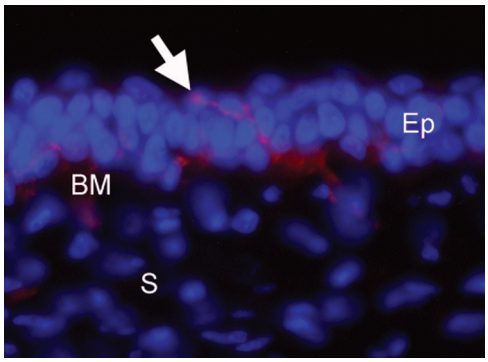

FIGURE 4. E16 10-μm frozen SV2-labeled section (*red*), Hoechst-stained nuclei (*blue*) with SV2-labeled punctate structures (*arrow*) in the corneal epithelium (Ep). BM, Bowman's membrane; S, stroma.

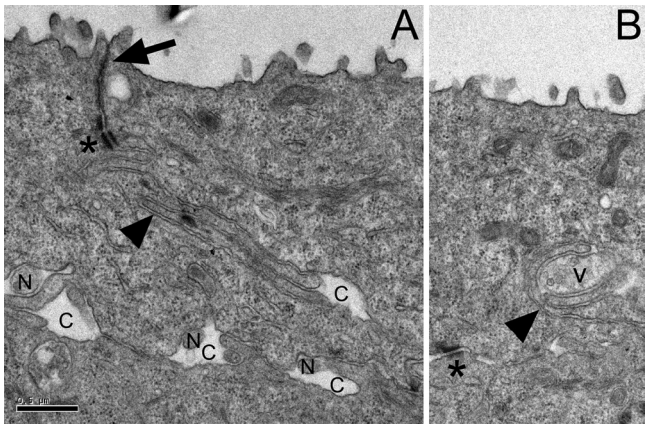

FIGURE 5. (**A**) EM of ACE cells with interdigitations (*arrowhead*) formed where two ACE abut, forming clefts (C) with corneal nerves (N) within clefts at the basolateral borders of ACE cells. Note tight junctions (*arrow*) and desmosomes (*asterisk*). (**B**) Vesicle-containing structure (V) within in interdigitation (*arrowhead*) between ACE cells. Scale bar, 0.5 μm.

microscopy. A striking characteristic of the ACE cells was that where two such cells abut one another they form extremely long interdigitations (Figs. 5A, B, arrowheads). These interdigitations were observed at all times examined (E12-E17). Some of them extended most of the way across both abutting cells, and many of them can be traced from the apical cell surface down to the basal surface. These interdigitations, at their apical surface, have tight junctions (arrow) that most likely form a barrier to the exterior environment, and along their lengths there are numerous desmosomes (Figs. 5A, B, asterisks). However, there are also regions in which the interdigitating membranes of the adjacent cells have obvious separations/clefts (Fig. 5A, [C]), showing that these are, in fact, intercellular channels. Near the basal region of the adjacent ACE cells, the separations/clefts become channels that are larger and more frequent. Here, they also contain nerves (n) and more complex structures that may represent the proposed synapse-like structures. In addition, near the basal region of the ACE cells, these channels connect with other channels that extend further downward to the base of the epithelial sheet and Bowman's layer (not shown).

As candidates for specialized, synapse-like structures, two general types of structures are observed within the intercellular clefts/channels, preferentially at the basolateral region. One type of structure consists of numerous clear core vesicles approximately 40 nm in diameter (Fig. 5B, v). The other type of structure also contains vesicles (Fig. 6A, arrow) but has another component that appears to consist of a nerve surrounded by alternating dark- and light-staining layers (Fig. 6A, arrowhead). These layers appear to be arranged in a jelly-roll fashion that is analogous to, but different from, the sheath of a myelinated nerve because corneal nerves are unmyelinated,[14] and myelin does not have dark- and light-staining components. Most of the surface of the jelly roll is freely exposed to the vesicle-containing cytoplasm within the cleft; however, one side is closely apposed or attached to the wall of the structure. This may be where the jelly roll is forming through an interaction between a nerve and the adjacent ACE cell or an associated Schwann cell (see Discussion). Consistent with these possibilities, there also exists a spectrum of similar, but less complex, structures (e.g., Figs. 6C–F), but whether these represent intermediates in the formation of more complex structures remains to be determined.

From their location it seemed likely that these structures, seen by EM, represent the synapse-like structures visualized by

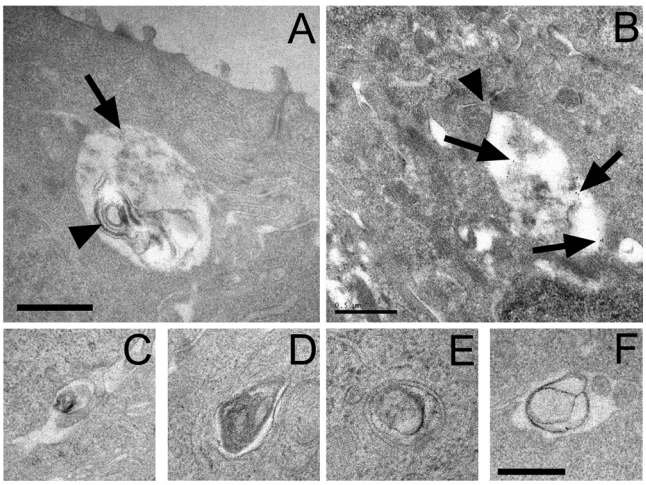

FIGURE 6. (**A**) EM of synapse-like structure with jelly roll–type formation (*arrowhead*) and vesicles (*arrow*). (**B**) Comparable structure to that of (**A**) within interdigitation (*arrowhead*) immunolabeled for SV2 by 10-nm gold particles (*arrows*). (**C–F**) EM of stages of synapse-like structures. Scale bars, 0.5 μm (**A**, **B**, **F**).

immunofluorescence with the TuJ-1 and SV2 antibodies. However, to verify this, we performed immunoelectron microscopy, using, as a marker, a colloidal gold-conjugated secondary antibody. However, it was found that fixatives containing glutaraldehyde could not be used because they destroyed antigenicity, but fixatives lacking this component failed to preserve membranous components such as vesicles. However, using the fixative described in Materials and Methods, we were able to determine that the structures that labeled with the SV2 colloidal gold (Fig. 6B, arrows), while lacking detail because of the suboptimal fixation, are the same type of structure as the one shown in Figure 6A because they are of the same size, organization, and location within the corneal epithelium.

Self-Propagation of TuJ-1$^+$ ACE Cells

The final, potentially novel property of the TUJ-1$^+$ ACE cells is that they are self-propagating. It is generally accepted that the suprabasal CE cells originate from basal cells, and it is in the basal layer that cell division occurs.[32] However, in our whole mount preparations reacted with the TuJ-1 antibody, we clearly detected a large number of TuJ-1$^+$ ACE cells that had TuJ-1-labeled mitotic figures (Fig. 7, arrows).

DISCUSSION

Origin of Corneal Nerves in the Chicken

Corneal nerves themselves are generally thought to be small-caliber, unmyelinated, nociceptive fibers that originate from the OTG and terminate in free nerve endings. However, in some species (e.g., rabbit and cat), at least a portion of the corneal nerves are derived from fibers originating in the SCG.[20] These fibers from the SCG are thought to be sympathetic, and it has been hypothesized that the sympathetic innervation of the cornea is involved in modulating ion transport[33] or modulating the sensitivity of the corneal sensory fibers.[34] However, it is unclear why in some species the cornea receives sympathetic innervation from the SCG and other species do not.

To determine the origin of corneal nerves in the chicken embryo, we performed retrograde labeling using the lipophilic dye DiI. The results are consistent with all the corneal nerves originating from pseudounipolar neurons whose cell bodies reside within the OTG because DiI-labeled cell bodies were found only in this ganglion and none were detected in any other cranial ganglia examined. In addition, in these assays, all the DiI-labeled cell bodies in the OTG were derived from corneal nerves because the dye was found throughout the corneal epithelium but none had spread to other tissues of the anterior eye. Results of these DiI-labeling experiments are consistent with CE cells and nerves being in close association with one another. For cell membranes, diffusion of DiI occurs only if the membranes are continuous or fused or if the cells are in close apposition (e.g., at junctions).[21] Corneal nerves were labeled by DiI placed on the surface of the corneal epithelium, suggesting that the dye diffused from CE cells to the nerve fibers, consistent with a close association between them. Although further physiological studies are necessary to verify such an association, morphologically we have observed structures that support this possibility.

Specialized Structures of Corneal Nerves

Polymodal nociceptors that transduce mechanical, thermal, and chemical noxious stimuli into sensations of pain, such as those that innervate the cornea, are generally thought to terminate as free nerve endings (i.e., they lack structural specializations).[35] However, certain sensory nerves do participate with epithelial cells in the formation of specialized structures, such as taste buds in the tongue and the pressure sensing Meissner's and Pacinian corpuscles of skin (reviewed by Watanabe[36]). For the cornea, two early ultrastructural studies on adult rabbit corneas have suggested that close relationships exist between corneal nociceptive nerve fibers and CE cells.[13,37] In addition, in human corneas it has been reported that at least some nociceptive endings have accumulations of small, clear vesicles.[14]

In the present study on the developing chicken cornea, we have obtained several lines of morphologic evidence supporting a close association between nerves and the ACE cells in the form of structures that we refer to as synapse-like. This term has been used previously by others in describing specialized endings that nerves make with epithelial cells in the peripheral nervous system and that share certain similarities with canonical synapses but may be morphologically distinct from them (reviewed by Kruger et al.[27]). In the developing chicken cornea, by EM these synapse-like structures range from those that consist of aggregations of small, clear vesicles to a variety of more complex profiles that, in addition to containing vesicles, also have a membranous component of one or more layers and structures that resemble synaptic densities. By EM these vesicles were shown to have characteristics of those associated with synapses (clear and measuring approximately 40 nm). In addition, the synapse-like structures in the cornea are immu-

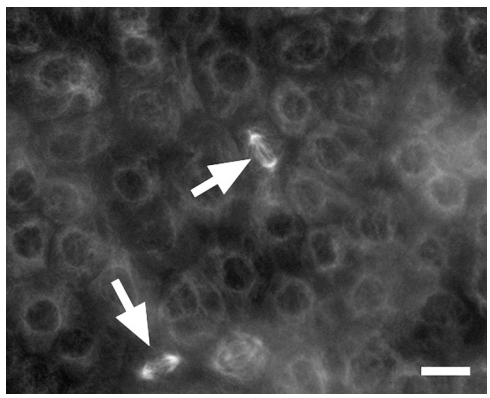

FIGURE 7. Whole mount E11 TuJ-1-labeled cornea imaged en face with mitotic figures (*arrows*). Scale bar, 10 μm.

nolabeled by the synaptic vesicle antibody (SV2), both by immunofluorescence and by immunoelectron microscopy.

There are a number of unknowns concerning these specialized nociceptive endings. Morphologically, we do not know whether the profiles shown in Figure 6 represent a variety of different type of structures or a single type of structure cut in different planes of section or at different stages of formation, nor do we know whether the membranous layer(s) is derived from the nerve itself or from an adjacent ACE cell or a Schwann cell.

TuJ-1$^+$ ACE: A Specialized Apical Corneal Epithelial Cell

In the process of analyzing corneal innervation using whole mount immunofluorescence with the TuJ-1 antibody, which is specific for class III (neuronal) β-tubulin, we observed that in addition to labeling nerves, ACE cells also showed immunoreactivity with the antibody. However, these cells, which we have termed TuJ-1$^+$ ACE cells, do have other characteristics of CE cells, such as the expression of cytokeratin K3 and nuclear ferritin and the nuclear ferritin transporter ferritoid.[38] These TuJ-1$^+$ ACE cells also have associated nerves, and these nerves have punctate densities that, on further analysis by electron and confocal microscopy, are likely to be the synapse-like structures described. That the TuJ-1 immunoreactivity within the TuJ-1$^+$ ACE cells is a product of this cell type and is not transported from the associated nerves is confirmed by the observation that the TuJ-1 staining of these cells appears at least 3 days before innervation occurs. That this immunoreactivity is to β-tubulin is confirmed by the observation that many TuJ-1$^+$ ACE cells are undergoing cell division and the mitotic figures of these show TuJ-1 labeling of the microtubules of the mitotic apparatus. Finally, that this tubulin is class III β-tubulin is strengthened by RT-PCR, indicating mRNA for this tubulin is present in CE tissue harvested before innervation has occurred. The expression of this isoform of β-tubulin outside the nervous system is rare but not unprecedented. A similar interaction between a TuJ-1-positive cell and associated nerves has been reported for Merkel cells in skin[39] and for certain rare, neuroendocrine cells in the developing lung and intestine.[40] Another similarity between these cell types and the corneal TuJ-1$^+$ ACE cells is that, in each of these cell types, the expression of class III β-tubulin is transient. For neuroendocrine cells, this occurs for only a short period during embryonic development. For corneal TuJ-1$^+$ ACE, immunofluorescence is first detected at E6 and remains at high levels until E16, after which no expression can be detected (JKK and TFL, unpublished observations, 2008).

Functionally, in the developing lung, these innervated, TuJ-1-positive neuroendocrine cells act as modulators of fetal lung growth and differentiation through the synthesis and secretion of neuropeptides and growth factors such as calcitonin gene-related peptide[41,42] (reviewed by Linnoila[43]). However, it is unclear what role or roles class III β-tubulin plays within these cell types during development and why its expression is transitory. For the β-tubulins in general, it has been suggested that the C-terminal amino acid sequence, which is specific for each isoform, alters the stability of the microtubules or allows for the biding of different microtubule-associated proteins and their functionality.[44] For now, however, this remains conjecture.

However, for the corneal TuJ-1$^+$ ACE cells, we have observed that one function is to participate in the mitotic apparatus of dividing cells. This observation is of interest for two reasons. The first is that, in the nervous system, the normal expression of class III β-tubulin is generally thought to occur in neurons before or just after their terminal mitosis.[45] However, for TuJ-1$^+$ ACE, cells this is unlikely to be the case because large numbers of TuJ-1-labeled mitotic figures are present between E7 and E16 (JKK and TFL, unpublished observations, 2008). The other interesting aspect of this observation is that it questions the finding that within the corneal epithelium, the only cells that undergo mitosis are those within the basal cell layer and that all suprabasal cells are derived from these in the adult cornea.[32] These results suggest that in the embryonic cornea, cell division occurs apically, in addition to basally, and they also suggest that these apical-most cells of the corneal epithelium represent a self-propagating population, at least during embryonic development, which again attests to the unique nature of these cells.

Acknowledgments

The authors thank Cathy Linsenmayer for expert assistance with electron microscopy and The Tufts Center for Neuroscience Research (P30 NS047243) for imaging support. The authors also thank Michele Jacob and James Schwob for antibodies and for helpful discussions.

References

1. Muller LJ, Marfurt CF, Kruse F, Tervo TMT. Corneal nerves: structure, contents and function. *Exp Eye Res.* 2003;76:521–542.
2. Beuerman RW, Schimmelpfennig B. Sensory denervation of the rabbit cornea affects epithelial properties. *Exp Neurol.* 1980;69:196–201.
3. Belmonte C, Acosta MC, Gallar J. Neural basis of sensation in intact and injured corneas. *Exp Eye Res.* 2004;78:513–525.
4. Bee JA. The development and pattern of innervation of the avian cornea. *Dev Biol.* 1982;92:5–15.
5. Clarke ND, Bee JA. Innervation of the chick cornea analyzed in vitro. *Invest Ophthalmol Vis Sci.* 1996;37:1761–1771.
6. Lwigale PY, Bronner-Fraser M. Lens-derived Semaphorin3A regulates sensory innervation of the cornea. *Dev Biol.* 2007;306:750–759.
7. Baker KS, Anderson SC, Romanowski EG, Thoft RA, SundarRaj N. Trigeminal ganglion neurons affect corneal epithelial phenotype: influence on type VII collagen expression in vitro. *Invest Ophthalmol Vis Sci.* 1993;34:137–144.
8. Garcia-Hirschfeld J, Lopez-Briones LG, Belmonte C. Neurotrophic influences on corneal epithelial cells. *Exp Eye Res.* 1994;59:597–605.
9. Chan KY, Haschke RH. Isolation and culture of corneal cells and their interactions with dissociated trigeminal neurons. *Exp Eye Res.* 1982;35:137–156.
10. Chan KY, Jones RR, Bark DH, Swift J, Parker JA Jr, Haschke RH. Release of neuronotrophic factor from rabbit corneal epithelium during wound healing and nerve regeneration. *Exp Eye Res.* 1987;45:633–646.
11. Netto MV, Mohan RR, Sinha S, Sharma A, Dupps W, Wilson SE. Stromal haze, myofibroblasts, and surface irregularity after PRK. *Exp Eye Res.* 2006;82:788–797.
12. Wilson SE, Ambrosio R. Laser in situ keratomileusis-induced neurotrophic epitheliopathy. *Am J Ophthalmol.* 2001;132:405–406.
13. MacIver MB, Tanelian DL. Free nerve ending terminal morphology is fiber type specific for A delta and C fibers innervating rabbit corneal epithelium. *J Neurophysiol.* 1993;69:1779–1783.
14. Muller LJ, Pels L, Vrensen GF. Ultrastructural organization of human corneal nerves. *Invest Ophthalmol Vis Sci.* 1996;37:476–488.
15. Hamburger V, Hamilton HL. A series of normal stages in the development of the chick embryo. *J Morphol.* 1951;88:49–92.
16. Fujimori KE, Takauji R, Yoshihara Y, Tamada A, Mori K, Tamamaki N. A procedure for in situ hybridization combined with retrograde labeling of neurons: application to the study of cell adhesion molecule expression in DiI-labeled rat pyramidal neurons. *J Histochem Cytochem.* 1997;45:455–459.
17. Linsenmayer TF, Eavey RD, Schmid TM. Type X collagen: a hypertrophic cartilage-specific molecule. *Pathol Immunopathol Res.* 1988;7:14–19.

18. Sillitoe RV, Hawkes R. Whole-mount immunohistochemistry: a high-throughput screen for patterning defects in the mouse cerebellum. *J Histochem Cytochem.* 2002;50:235–244.
19. Spurr SJ, Gipson IK. Isolation of corneal epithelium with dispase II or EDTA: effects on the basement membrane zone. *Invest Ophthalmol Vis Sci.* 1985;26:818–827.
20. Marfurt CF, Kingsley RE, Echtenkamp SE. Sensory and sympathetic innervation of the mammalian cornea: a retrograde tracing study. *Invest Ophthalmol Vis Sci.* 1989;30:461–472.
21. Baker GE, Reese BE. Using confocal laser scanning microscopy to investigate the organization and development of neuronal projections labeled with DiI. *Methods Cell Biol.* 1993;38:325–44.:325–344.
22. Lee MK, Tuttle JB, Rebhun LI, Cleveland DW, Frankfurter A. The expression and posttranslational modification of a neuron-specific beta-tubulin isotype during chick embryogenesis. *Cell Motil Cytoskeleton.* 1990;17:118–132.
23. Fanarraga ML, Avila J, Zabala JC. Expression of unphosphorylated class III beta-tubulin isotype in neuroepithelial cells demonstrates neuroblast commitment and differentiation. *Eur J Neurosci.* 1999; 11:517–527.
24. Horton S, Meredith A, Richardson JA, Johnson JE. Correct coordination of neuronal differentiation events in ventral forebrain requires the bHLH factor MASH1. *Mol Cell Neurosci.* 1999;14:355–369.
25. Sullivan KF, Havercroft JC, Machlin PS, Cleveland DW. Sequence and expression of the chicken beta 5- and beta 4-tubulin genes define a pair of divergent beta-tubulins with complementary patterns of expression. *Mol Cell Biol.* 1986;6:4409–4418.
26. Hasegawa S, Miyoshi Y, Egawa C, et al. Prediction of response to docetaxel by quantitative analysis of class I and III beta-tubulin isotype mRNA expression in human breast cancers. *Clin Cancer Res.* 2003;9:2992–2997.
27. Kruger L, Light AR, Schweizer FE. Axonal terminals of sensory neurons and their morphological diversity. *J Neurocytol.* 2003;32: 205–216.
28. Haeberle H, Fujiwara M, Chuang J, et al. Molecular profiling reveals synaptic release machinery in Merkel cells. *Proc Natl Acad Sci U S A.* 2004;101:14503–14508.
29. Bindra PS, Knowles R, Buckley KM. Conservation of the amino acid sequence of SV2, a transmembrane transporter in synaptic vesicles and endocrine cells. *Gene.* 1993;137:299–302.
30. Bajjalieh SM, Frantz GD, Weimann JM, McConnell SK, Scheller RH. Differential expression of synaptic vesicle protein 2 (SV2) isoforms. *J Neurosci.* 1994;14:5223–5235.
31. Hrabovszky E, Deli L, Turi GF, Kallo I, Liposits Z. Glutamatergic innervation of the hypothalamic median eminence and posterior pituitary of the rat. *Neuroscience.* 2007;144:1383–1392.
32. Beebe DC, Masters BR. Cell lineage and the differentiation of corneal epithelial cells. *Invest Ophthalmol Vis Sci.* 1996;37:1815–1825.
33. Klyce SD, Beuerman RW, Crosson CE. Alteration of corneal epithelial ion transport by sympathectomy. *Invest Ophthalmol Vis Sci.* 1985;26:434–442.
34. Morgan C, DeGroat WC, Jannetta PJ. Sympathetic innervation of the cornea from the superior cervical ganglion: an HRP study in the cat. *J Auton Nerv Syst.* 1987;20:179–183.
35. Fox EA, Phillips RJ, Martinson FA, Baronowsky EA, Powley TL. Vagal afferent innervation of smooth muscle in the stomach and duodenum of the mouse: morphology and topography. *J Comp Neurol.* 2000;428:558–576.
36. Watanabe IS. Ultrastructures of mechanoreceptors in the oral mucosa. *Anat Sci Int.* 2004;79:55–61.
37. Tanelian DL, MacIver MB. Simultaneous visualization and electrophysiology of corneal A-delta and C fiber afferents. *J Neurosci Methods.* 1990;32:213–222.
38. Beazley KE, Nurminskaya M, Talbot CJ, Linsenmayer TF. Corneal epithelial nuclear ferritin: developmental regulation of ferritin and its nuclear transporter ferritoid. *Dev Dyn.* 2008;237:2529–2541.
39. Lucarz A, Brand G. Current considerations about Merkel cells. *Eur J Cell Biol.* 2007;86:243–251.
40. Katsetos CD, Herman MM, Mork SJ. Class III beta-tubulin in human development and cancer. *Cell Motil Cytoskeleton.* 2003;55:77–96.
41. Li K, Nagalla SR, Spindel ER. A rhesus monkey model to characterize the role of gastrin-releasing peptide (GRP) in lung development: evidence for stimulation of airway growth. *J Clin Invest.* 1994;94:1605–1615.
42. White SR, Hershenson MB, Sigrist KS, Zimmermann A, Solway J. Proliferation of guinea pig tracheal epithelial cells induced by calcitonin gene-related peptide. *Am J Respir Cell Mol Biol.* 1993; 8:592–596.
43. Linnoila RI. Functional facets of the pulmonary neuroendocrine system. *Lab Invest.* 2006;86:425–444.
44. Joshi HC, Cleveland DW. Differential utilization of beta-tubulin isotypes in differentiating neurites. *J Cell Biol.* 1989;109:663–673.
45. Dennis K, Uittenbogaard M, Chiaramello A, Moody SA. Cloning and characterization of the 5′-flanking region of the rat neuron-specific Class III beta-tubulin gene. *Gene.* 2002;294:269–277.